caused by mist events and mist and rain events (which could not be separated). The highest attenuation part of the distribution follows a –1/2(dB/km)/decade slope for the low percentages of time. Highest attenuation values recorded during the measurement period were never > 13dB/km, which is comparable with the results of Chu and Hogg [1] for a 2.6km, 0.63μm path. Fig. 2 presents the cumulative distribution of attenuation for rainfall/mist events only. The highest attenuation part of the distribution follows a 2/3(dB/km)/decade. The season for greatest attenuation was found to be the winter, when mist, very often accompanies rainfall.

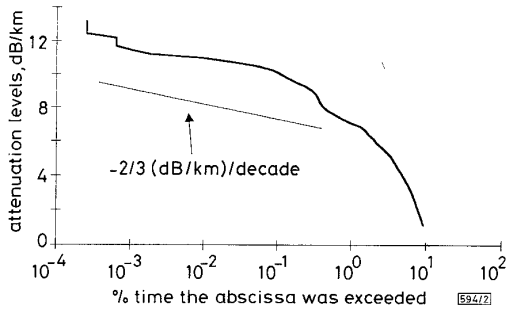

Fig. 2 *Cumulative probability distribution function of attenuation caused only by combination of rain and mist for period covering autumn 1993 to summer 1994*

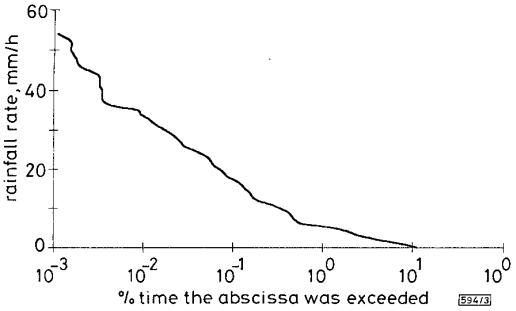

Fig. 3 *Cumulative probability distribution function of rainfall for period covering autumn 1993 to summer 1994*

Fig. 3 shows the rainfall cumulative distribution function for the same year. The point measurement of the rainfall rate can cause imprecision in real time correlation between attenuation and rainfall rate because it will not necessarily represent the rainfall rate on the 4.1km path. A statistical approach is used in which the percentiles of the distributions in Figs. 2 and 3 are compared to obtain the relationship between attenuation and rainfall rate. The relationship between attenuation (A) and rainfall rate (R) is usually represented in the form $A = aR^b$ [2]. This expression does not make any allowance for mist present on the path. However, the results of this work produced a very good fit to this expression,

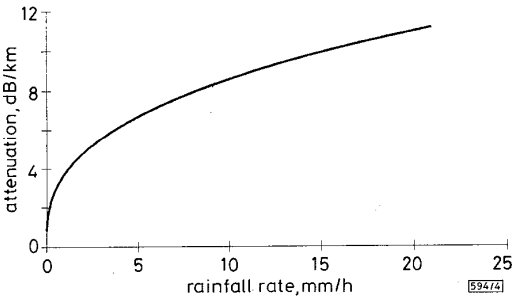

Fig. 4 *Relationship between attenuation and rainfall for period covering autumn 1993 to summer 1994*

$A = 3.749R^{0.3586}$
Correlation coefficient = 0.9173

with a correlation coefficient of 0.92. Values derived for the parameters a and b were 3.75 and 0.36, respectively. The percentiles of the distributions were obtained by fitting curves to the empirical distributions. A piecewise linear fit was used for the distribution of attenuation, and an exponential fit was used for the distribution of rainfall. Fig. 4 shows the diagram of the percentiles of attenuation against the percentiles of rainfall rate obtained in this way. The values of the parameters a and b obtained were quite different to those obtained by Gibbins *et al.* [3], which were ~2 and 0.6, respectively. However, their measurements were for rainfall only. The discrepancy is to be expected as the results are not comparable. The attenuation measured in this work is not only caused by rainfall but includes the very practical case of the presence of mist. Also, the single measurement of rainfall rate is not necessarily indicative of the rainfall rate along the path.

Conclusions: Cumulative distributions of attenuation and rainfall rate were obtained for one year of measurements on a 4.1km line of sight link operating at 1.55μm. Winter was found to be the worst season for attenuation, in part caused by the mist occurring simultaneously to rain. The maximum attenuation found was 13dB/km. Results for the twelve months data of attenuation (A) against rainfall rate (R) exhibited a close fit to the relation $A = aR^b$.

Acknowledgments: Thanks are due to BT Laboratories, Martlesham Heath, Ipswich, which loaned the 1.55μm equipment. Thanks are also due to the Brazilian National Research Council, CNPq, Brazil, for financial support to E. Couto de Miranda.

24 November 1995
Electronics Letters Online No: 19960215

E. Couto de Miranda and R.S. Cole (*Department of Electronic and Electrical Engineering, University of London, Torrington Place, London WC1E 7JE, United Kingdom*)

D.R. Wisley and P.L. Eardley (*British Telecom Laboratories, Martlesham Heath, Ipswich, Suffolk, IP5 7RE, United Kingdom*)

References

1 CHU, T.S., and HOGG, D.C.: 'Effects of precipitation on propagation at 0.63, 3.5 and 10.5 microns', *Bell Syst. Tech. J.*, 1968, **46**, pp. 723–759

2 OLSEN, R.L., ROGERS, D.V., and HODGES, D.B.: 'The aR^b relation in the calculation of rain attenuation', *IEEE Trans.*, 1978, **AP-26**, pp. 318–329

3 GIBBINS, C.J.: 'Statistical studies of propagation and related meteorology over a 500m path'. IEEE Int. Conf. Antennas Propag., York, 1991, pp. 673–676

Space-switching 2.5Gbit/s signals using wavelength conversion and phased array routing

A.A.M. Staring, L.H. Spiekman, C. van Dam, E.J. Jansen, J.J.M. Binsma, M.K. Smit and B.H. Verbeek

Indexing terms: High-speed optical techniques, Optical switches, Optical communication

Space switching of 2.5Gbit/s optical signals by wavelength conversion in a DBR laser and subsequent routing through a phased array wavelength demultiplexer is demonstrated. In addition, first results are presented using an integrated chip consisting of a phased array with 3dB couplers at its inputs.

Introduction: Space switching of high-speed optical signals is a key towards the realisation of flexible all-optical networks. Using a matrix of 2 × 2 switches (e.g. Mach-Zehnder or DOS type) an $N \times N$ optical switch can be constructed. However, the complexity of such a circuit increases with N^2 [1].

Exploitation of the wavelength domain allows construction of switches having a complexity that increases linearly with N. In this

concept, tunable wavelength converters are used in combination with wavelength routing to link inputs and outputs. A straightforward approach is to combine the converted input signals in a star coupler and apply fixed wavelength filters at the outputs [2]. In this fashion, however, most of the available signal power is discarded in the filters.

Here, we employ an $N \times N$ phased array wavelength demultiplexer (PHASAR) for routing, removing the need for optical filters. The concept is first demonstrated using discrete components. Next, experiments are presented using a partly integrated solution.

Experimental: To test the concept, the setup shown in Fig. 1 has been built using discrete components. The heart of the space switch is formed by a polarisation-insensitive 8 × 8 PHASAR [3]. The channel spacing is 2nm, with a crosstalk between channels of less than –25dB. Using two lensed fibres to route the signal through the chip, a fibre-to-fibre loss of 13dB is obtained.

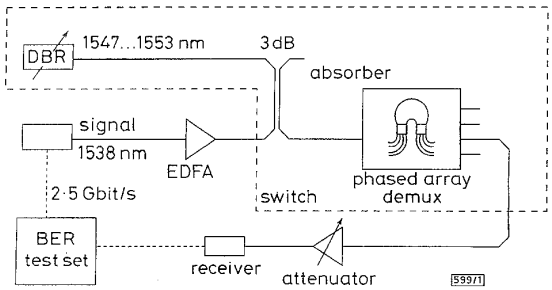

Fig. 1 *Demonstration of space switching with PHASAR, DBR wavelength converter and 3dB coupler*

For the experimental demonstration, only a single wavelength converter and signal source have been used. The wavelength converter is a current-injection tunable DBR laser with an 8nm tuning range [4], which is sufficiently large to address four of the PHASAR channels. About +4dBm of CW output power is injected into a lensed fibre at a gain current of 65mA.

The signal source is a DFB laser emitting at 1538nm, modulated at a rate of 2.5Gbit/s with a pseudorandom bit sequence (PRBS) of length 2^{23}–1, using a 40mA peak-to-peak drive current. To compensate for coupling losses, the laser signal power is amplified by an EDFA with adjustable gain (+18dBm maximum output power).

A fused-fibre 3dB coupler is used to connect the PHASAR, DBR and signal source as shown in Fig. 1. The light from the PHASAR output of choice is fed through an adjustable attenuator, and subsequently detected by a 2.5Gbit/s receiver.

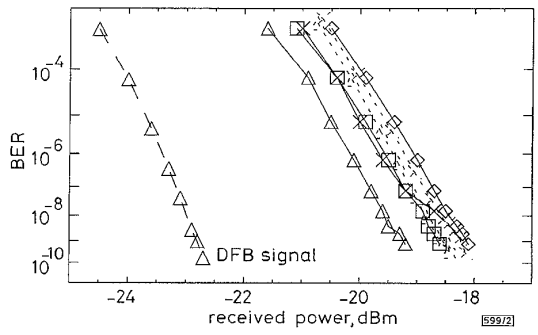

Fig. 2 *BER measurements of input, converted and routed signals*

λ 1546.6, 1548.6, 1550.6 and 1552.6nm, routed
– – – – λ = 1538nm, input
- - - - - converted
◇ Ch1, △ Ch2, □ Ch3, × Ch4

Fig. 2 shows the results of bit error rate (BER) measurements, with approximately +11.5dBm of signal power delivered to the DBR. The curves of four states of the switch have been obtained by electronically tuning the DBR to the appropriate wavelength, and adjusting the outcoupling fibre tip position. A receiver sensitivity of –23.5dBm (at a BER of 10^{-9}) is obtained for the DFB input signal. From the Figure it is clear that wavelength conversion plus space switching using this configuration results in a penalty of 4.5dB. By detecting the converted signal without routing through the PHASAR, it is found that this penalty is entirely due to the wavelength conversion process. (For this experiment, a bulk-optic tunable bandpass filter is used in order to remove the DFB signal at 1538nm which is reflected from the front facet of the DBR laser.)

The first step towards a fully integrated space switch is to integrate all passive components on a single chip. Such a chip has been fabricated for the second part of the experiments, using the same technology [3] as for the PHASAR discussed above. It only needs connection of DBR wavelength converters to yield a complete 4 × 4 space switch.

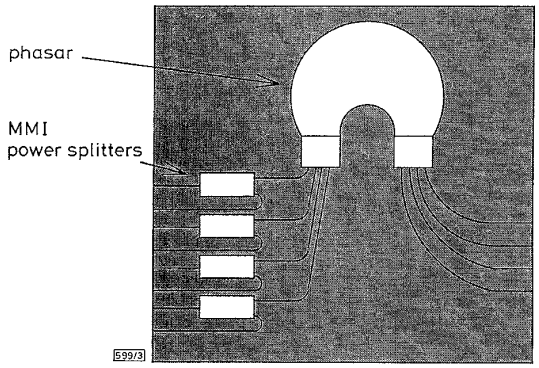

Fig. 3 *Schematic layout of InGaAsP chip containing polarisation independent PHASAR and MMI power splitters*

The PHASAR on the integrated chip has a channel spacing of 1 nm. As shown in Fig. 3, the inputs of the PHASAR are equipped with power splitters based on the multimode interference (MMI) effect [5]. The in- and outputs have been given a pitch of 250μm, in order to facilitate coupling with arrays of lensed fibres. Total chip size is 3 × 5mm.

Measurements have been made using a setup similar to the one shown in Fig. 1. The main difference is that a photodetector and sampling scope are used instead of the receiver and BER tester. In this configuration, the signal has to cross three fibre-chip couplings as against only one in the previous setup. Combined with a slightly higher on-chip propagation loss, this results in delivery of only +2.5dBm of signal power to the DBR.

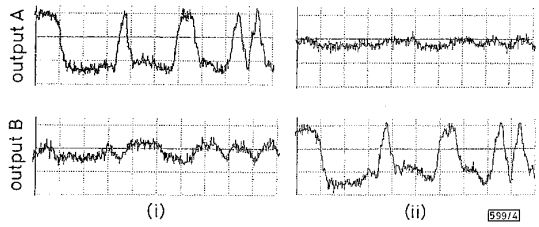

Fig. 4 *Signal at two outputs of space switch*

256 × averaged, λ_{input} = 1538nm
(i) λ_{DBR} = 1548.1nm
(ii) λ_{DBR} = 1549.1nm

Fig. 4 shows a part of the bit pattern detected by the photodetector at two outputs, clearly showing space switching behaviour. The structure observed in the lower left trace is caused by scattered light from the high power (+18dBm) input signal.

Discussion: The sensitivities obtained for the four channels of the switch used in the first part of the experiments are uniformly distributed. Owing to degradation of the extinction ratio of the converted signal, a BER penalty of 4.5dB is observed. The main reason for this degradation is that an off-the-shelf DBR laser with uncoated front facet has been used. A considerable reduction of the input power requirements and improvement of the extinction

ratio can be obtained by applying a low reflectivity coating to this facet [6]. Operating the DBR closer to threshold also improves the extinction ratio of the converted signal, but at the expense of available output power.

While large improvements can be made by optimising the DBR laser, the main disadvantage of this configuration is that three fibre-chip couplings are necessary for the signal to reach the wavelength converters. This can be solved by integrating the DBR laser on-chip. However, because of easier integration with the PHASAR, wavelength conversion by means of an asymmetric MZI configuration with SOAs [7] might be a more viable approach. In this case the DBR lasers are used as tunable CW sources feeding the wavelength converters with the new signal wavelength.

Conclusion: A 4-channel space switch has been demonstrated by combining a phased array wavelength demultiplexer and a tunable DBR wavelength converter. Due to the nonoptimised DBR laser, BER measurements exhibit a 4.5dB penalty. In addition, an InGaAsP chip has been fabricated integrating the phased array router and power splitters at its inputs. Space-switching has been clearly oberved for this chip, which only needs connection of DBR wavelength converters to form a complete space switch.

Acknowledgments: The authors wish to thank C. K. Wong for providing the 2.5Gbit/s receiver, and F. Willems (AT&T Network Systems, The Netherlands) for use of a high output power EDFA.

15 December 1995

Electronics Letters Online No: 19960196

A.A.M. Staring, E.J. Jansen, J.J.M. Binsma and B.H. Verbeek (*Philips Optoelectronics Centre, Prof. Holstlaan 4, 5656 AA Eindhoven, The Netherlands*)

L.H. Spiekman, C. van Dam and M.K. Smit (*Department of Electrical Engineering, Delft University of Technology, The Netherlands*)

References

1 OKUNO, M., KATOH, K., SUZUKI, S., OHMORI, Y., and HIMENO, A.: 'Strictly nonblocking 16x16 matrix switch using silica-based planar lightwave circuits'. Proc. 20th Euro. Conf. Opt. Comm. (ECOC'94), Florence, 25–29 September 1994, Post-deadline papers, pp. 83–86

2 GABRIAGUES, J.M., and JACOB, J.B.: 'Exploitation of the wavelength domain for photonic switching in the IBCN'. Proc. 17th Euro. Conf. Opt. Comm. (ECOC'91), Paris, 9–12 September 1991, Invited papers, pp. 59–66

3 VERBEEK, B.H., STARING, A.A.M., JANSEN, E.J., VAN ROIJEN, R., BINSMA, J.J.M., VAN DONGEN, T., AMERSFOORT, M.R., VAN DAM, C., and SMIT, M.K.: 'Large bandwidth polarisation independent and compact 8 channel PHASAR demultiplexer/filter'. OFC/IOOC'94 Tech. Dig., San Jose, CA, 20–25 February 1994, Post-deadline papers, pp. 63–66

4 STARING, A.A.M., BINSMA, J.J.M., KUINDERSMA, P.I., JANSEN, E.J., THIJS, P.J.A., VAN DONGEN, T., and DEPOVERE, G.F.G.: 'Wavelength-independent output power from an injection-tunable DBR laser', *IEEE Photonics Technol. Lett.*, 1994, **6**, pp. 147–149

5 SOLDANO, L.B., BOUDA, M., SMIT, M.K., and VERBEEK, B.H.: 'New small-size single-mode optical power splitter based on multi-mode interference'. Proc. 18th Euro. Conf. Opt. Comm. (ECOC'92), Berlin, 27 September–1 October 1992, pp. 465–468

6 BRAAGAARD, C., MIKKELSEN, B., DURHUUS, T., and STUBKJAER, K.E.: 'Modelling the DBR laser used as wavelength conversion device', *J. Lightwave Technol.*, 1994, **12**, pp. 943–951

7 VODJANI, N., RATOVELOMANANA, F., ENARD, A., GLASTRE, G., RONDI, D., BLONDEAU, R., DURHUUS, T., JOERGESEN, C., MIKKELSEN, B., STUBKJAER, K.E., PAGNOD, P., and BAETS, R.: 'All optical wavelength conversion at 5Gbit/s with monolithic integration of semiconductor optical amplifiers in a passive asymmetric Mach-Zehnder interferometer'. Proc. 20th Euro. Conf. Opt. Comm. (ECOC'94), Florence, 25–29 September 1994, Post-deadline papers, pp. 95–98

Time evolution measurement of zero dispersion wavelength in an installed submarine optical amplifier system

M. Murakami, T. Takahashi, M. Aoyama and M. Amemiya

Indexing terms: Optical communication, Optical fibre dispersion

Time evolution of zero dispersion wavelength was measured over 9000 km in an installed optical amplifier transmission system with dispersion managed submarine cables. The measured result shows that the system has sufficient stability for high speed transmission: the standard deviation of zero dispersion wavelength is <0.022 nm.

Introduction: Chromatic dispersion must be carefully managed in long-haul optical amplifier transmission systems, because the dispersion induced degradation accumulates along the system and is enhanced significantly by fibre nonlinearity [1]. In such systems, the average zero dispersion wavelength (ZDW) of the whole system should agree with the signal wavelength with subnanometer accuracy, if the bit rate is over several Gbit/s. Even if successfully managed, the ZDW of an installed submarine cable may fluctuate due to pressure, temperature and strain changes according to the undersea environment [2]. Therefore, it is necessary to test the ZDW-stability of a high speed optical amplifier system to ensure the system's transmission performance.

In this Letter, we report, for the first time, the results of time evolution measurements of the average ZDW of an installed optical amplifier system which was constructed with properly dispersion managed submarine cables [3]. The results of our measurements will be discussed with regard to the waveform distortion experienced in high speed, long distance transmission.

Experiment: The measured system consisted of the optical amplifiers and submarine cables laid between Kagoshima and Okinawa; the system length is 900km with 90km repeater spacing [3]. The water depth diagram of the route is shown in Fig. 1*a*. Almost half the route had a depth of over 1000m with a maximum depth of 3600m.

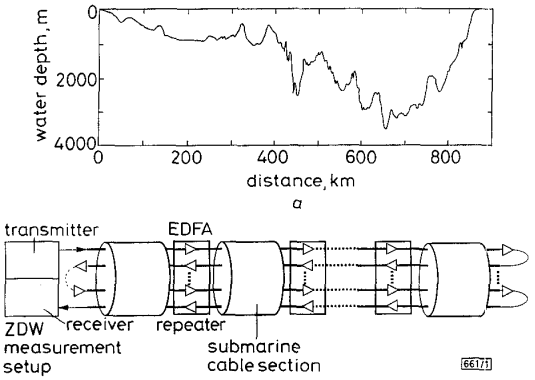

Fig. 1 *Water depth variation along route and experimental configuration*

a Water depth variation
b Experimental configuration

Each section of the submarine cable was composed of 12 dispersion-shifted-fibres covered with a trisected steel pipe, and low and high density polyethylene sheathes. Nonarmored cable was used in deep water, while armored cable was used in the shallow water near the shore where the risk of damage was considered to be significant. The overall average dispersion of each line was adjusted to be zero at around 1552.0nm, while the local dispersion value at the input end of each cable section was made negative to reduce the excess noise that is induced by the fibre nonlinearity. The average fibre loss was 0.21dB/km. The average optical output power from each repeater was controlled to be 6dBm [3]. We concatenated each up and down 900km line with a looped back configuration to build a transmission line of 9000km as shown in Fig. 1*b*.